International Scholarly Research Network
ISRN Renewable Energy
Volume 2012, Article ID 203149, 13 pages
doi:10.5402/2012/203149

Research Article

Solar Potential in the Himalayan Landscape

T. V. Ramachandra,[1,2,3] Gautham Krishnadas,[1] and Rishabh Jain[1]

[1] *Energy & Wetlands Research Group, Center for Ecological Sciences (CES), Indian Institute of Science, Karnataka, Bangalore 560012, India*
[2] *Centre for Sustainable Technologies (ASTRA), Indian Institute of Science, Karnataka, Bangalore 560012, India*
[3] *Centre for Infrastructure, Sustainable Transportation and Urban Planning (CiSTUP), Indian Institute of Science, Karnataka, Bangalore 560012, India*

Correspondence should be addressed to T. V. Ramachandra, cestvr@ces.iisc.ernet.in

Received 11 October 2011; Accepted 2 November 2011

Academic Editors: J. Kaldellis, M. Muselli, and A. Parretta

Estimation of solar energy reaching the earth's surface is essential for solar potential assessment. Solar radiation data based on satellites provide higher spatial and temporal coverage of regions compared to surface based measurements. Solar potential of the Indian hill state of Himachal Pradesh has been assessed using reliable satellite based global horizontal insolation (GHI) datasets validated based on its complex terrain. Solar maps representing regional and temporal resource availability in the state have been generated using geographical information systems (GIS). Spatial analyses show that the state receives annual average GHI above 4.5 kWh/m^2/day and a total of 99530395 million kWh (or million units, MU). The regional availability of GHI in Himachal Pradesh is influenced by its eclectic topography, seasons as well as microclimate. The lower and middle elevation zone (<3500 m) with tropical to wet-temperate climate receives higher GHI (>5 kWh/m^2/day) for a major part of the year compared to the higher elevation zone (>3500 m) with dry-temperate to alpine climate (4–4.5 kWh/m^2/day). Results show that Himachal Pradesh receives an average insolation of 5.86 ± 1.02–5.99 ± 0.91 kWh/m^2/day in the warm summer months; 5.69 ± 0.65–5.89 ± 0.65 kWh/m^2/day in the wet monsoon months; 3.73 ± 0.91–3.94 ± 0.78 kWh/m^2/day in the colder winter months.

1. Introduction

Energy plays a pivotal role in the development of a region. However, energy shortages in recent times, the imminent energy crisis, and threat of climate change have focused the attention for a viable sustainable alternative through renewable sources of energy. Sun being the vital source of renewable energy manifested in different forms in the solar system; it is necessary to understand the mechanism of energy flow involved. The geometry of the earth-sun movements causes large spatial, diurnal, and seasonal variations in the amount of solar radiation received on earth. The 23.5° tilt of the earth's rotational axis with respect to the plane of orbital revolution causes larger annual variations near the poles and smaller variations near the equator [1]. Due to the variations in the sun-earth distance, intercepted solar radiation fluctuates by ±3.3% around its mean value. The variations, due to sunspots, prominences and solar flares, can be neglected as they constitute small fraction compared to the total energy emitted by the sun. The average solar radiation falling on the earth's atmosphere called the solar constant is estimated to be 1.36 kW/m^2. The presence of clouds, suspended dust, gas molecules, and aerosols in the atmosphere, through absorption and scattering, attenuates the incident solar energy radiation (also called insolation). A fraction of 0.3 of the total incident solar energy called the albedo of the earth-atmosphere system is reflected back to the space [2]. The remaining fraction of solar energy in the form of direct and diffuse insolation which comprises the global horizontal insolation (GHI) is utilized in many processes like heating and illuminating the earth, photosynthesis, growth of vegetation, evapotranspiration, and snow ablation as well as solar-energy-based applications.

Solar radiation data is essential for designing solar-energy based applications as it is for meteorology, climatology, oceanography, agriculture, forestry, and other domains.

Solar energy applications like photovoltaic based-off-grid and grid-connected power generation, solar water heaters, thermal concentrators, solar cookers, desalination plants, passive building heating, and so forth demand reliable information on GHI at different regions of interest. This could be estimated from insolation data procured from on-ground pyranometric network, models based on meteorological parameters or those based on satellite data.

1.1. Solar Potential Assessment

1.1.1. Insolation Data from Pyranometric Network. Conventionally, solar potential of a region is assessed using the insolation data obtained from ground-based radiation stations. There are 572 radiation stations around the world which provide global, diffuse, and direct insolation data on hourly, daily, or monthly basis to the World Radiation Data Centre (WRDC) apart from other archived data [3]. An efficient and reliable pyranometric network incurs heavy investment in terms of capital, maintenance, and manpower. Developing countries like India, with a vast land area of 3287263 km^2, find it hard to have a sufficient spatial coverage for insolation measurements. The Indian radiation network under the Indian Meteorological Department (IMD) has merely 44 radiation stations spread across the country. Data from ground-based solar-radiation-monitoring stations are liable to errors due to calibration drift, manual data collection, soiling of sensors, and nonstandardization of measuring instruments [4]. The World Climate Research Program in 1989 had estimated a cumulative uncertainty of 6%−12% in measurements from conventional solar-monitoring stations [5]. Most of the data available from radiation stations are at nonuniform and interrupted periods as shown by Ortega et al. [6] for Chile which was reported to be 3 months to 21 years. Measurement uncertainties are below 3% at certain research-class sites meant for atmospheric or precision studies, but these are exceptions [7]. The radiation network in India expanded from 4 stations in 1957 to 44 as of today, measuring one or more parameters like global, direct, or diffuse radiation at different locations. These datasets provide temporal information (in minutes) which is essentially important for solar energy applications and design. Annual insolation varies with change in angle of incidence of the solar radiation. It is reported that a minimum of 7–10 years of solar radiation data are required to get a long-term mean within 5% [8].

1.1.2. Insolation Data from Meteorological Parameters. Insufficient insolation data, consequent to sparse radiation networks, lead to different parametric (Iqbal and ASHRAE model) and decomposition models (Angstrom, Hay, Liu and Jordan, Orgill and Hollands model). These models employ theoretical or empirical methods for interpolation or extrapolation of measured meteorological values to derive insolation data [1]. These models use parameters like sunshine duration [9, 10], temperature [11], rainfall [12], cloud cover [13], extraterrestrial radiation [14], and so forth for estimating solar radiation over a given location. Artificial neural networks (ANNs) are also being utilized for deriving insolation data based on climatological and geographical parameters [15]. These methods show low relative root mean square errors (RRMSEs) of 5% on validation with in-situ measurements.

1.1.3. Insolation Data from Satellites. Remote sensing data from polar satellites at ∼850 km with higher spatial resolution and geostationary satellites at ∼36000 km with higher temporal resolution are being utilized for estimation of insolation based on different subjective, empirical, and theoretical methods [16, 17]. Subjective methods involve subjective interpretation of cloud cover from the satellite images and its statistical relationship with atmospheric transmittance. Empirical methods depend on functional relations based on satellite-derived data and available solar radiation data which are customized for any place and time. Empirical methods are classified into two models: statistical and physical. Another method which simulates radiant energy exchanges taking place within the earth atmospheric system, hypothetically not demanding empirical calibration of model parameters, is called theoretical method. The broadband and spectral models are attached to this method [18].

The solar potential of Kampuchea was estimated based on a statistical model [19] with the visible and infrared images obtained from the Japanese Stationary Meteorological Satellite GMS-3 along with ground-based regression parameters and concluded that seasonal average of daily insolation depended more on the topography of the region than on seasonal variations. The RRMSE of the monthly average insolation was shown to vary from 5.7% to 11.6% with the mean of ground values as the cloudiness of the region increased. The solar potential of Pakistan was estimated by employing a physical model [17] based on the images collected from the Geostationary Operational Environmental Satellite (GOES) INSAT which scanned the region four times per day. The results indicated that the desert and plateau regions received favourable GHI while the monsoon had its influence on reduced insolation in the Eastern and Southeastern Pakistan, for the months of August, October, and May.

The daily direct and global insolation in 6 locations of India (from 2000 to 2007) was estimated based on a statistical model using Meteosat images of 5×5 km spatial resolution addressing the aerosol component in the atmosphere. These were validated against the surface global insolation for 5 locations with a RRMSE of 12% [20]. Stretched-Visible Infrared Spin Scan Radiometer (S-VISSR) images of the Geostationary Meteorological Satellite (GMS) of 15-minute interval high spatial resolution ($0.01^\circ \times 0.01^\circ$) for a period of 3 months in 1996 [21] were analysed to develop a bispectral threshold technique with respect to earth-atmosphere albedo and infrared temperature. The RRMSE with respect to ground data from 67 weather stations was calculated to be 25% for hourly and 12% for daily insolation. Similar endeavor generated hourly and monthly basis global as well as direct insolation maps using the SOLARMET physical model applied over 7 years high-resolution Meteosat satellite images [22]. A physical model based on visible-range satellite images considering the climatological aspects of hourly GHI

Figure 1: Study area—Himachal Pradesh, India.

useful for designing solar energy systems was designed [23], and monthly average hourly insolation datasets with RMSE ~10% when validated with 25 pyranometric stations were obtained. The extent of high solar resource availability zones in India was quantified on the basis of NASA SSE GHI data, and power generation potential of concentrated and photovoltaic applications was demonstrated in the wake of encouraging solar policies in the country [24].

Satellite-data-based models do not show much difference in performance as the primary source of ambiguity for all these models is the influence of cloud pattern. It has been proved that interpolations and extrapolations of available ground data for predicting solar radiation over distances beyond 34 km show higher RMSE compared to satellite-data-based measurements [25]. RMSEs for different models have been found to be within 20% for hourly values and 10% for daily values [26]. Today satellite data for about 20 years are available, which reduces the possibility of error due to annual variations in insolation. Nevertheless, ground data is indispensable at this juncture for validation and model improvement of satellite-based data.

2. Objectives of the Study

The objectives of this study are (i) to analyze the available satellite-based high-spatiotemporal-resolution insolation data and (ii) to employ them to assess the solar potential of Indian federal state of Himachal Pradesh representing a complex Himalayan terrain with scanty surface measurements.

3. Study Area

3.1. Geography and Climate. Himachal Pradesh (Figure 1) is located from 30.38° to 33.21° North latitudes and 75.77° to 79.07° East longitudes in the western Himalayas, covering a geographical area of 55673 km^2. The state is divided into 12 districts surrounded by Jammu & Kashmir in the North, Tibet in the Northeast, Uttarakhand in East/Southeast, Haryana in South, and Punjab in Southwest/West, with an abundance of snow-fed perennial rivers and rivulets. Out of the total area, 37033 km^2 is managed by the Forest department and 16376 km^2 is under permanent snow cover [27].

The agroclimatic zones of Himachal Pradesh are classified based on its elevation above mean sea level and related biogeography. Parts of Una, Bilaspur, Hamirpur, Kangra, Solan and Sirmaur districts in the Western and Southern regions lie below 1000 m with a tropical to subtropical climate and respective vegetation. Some portions of Solan, Sirmaur, Mandi, Chamba, and Shimla districts at altitude between 1000 and 3500 m have climate conditions varying from subtropical to wet-temperate with elevation. Lahaul Spiti, Kullu, and Kinnaur districts ranging between 3500 and 6700 m are part of the dry-temperate, subalpine and

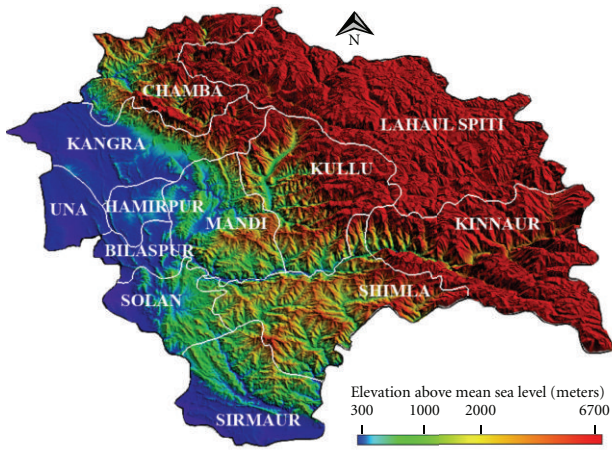

Figure 2: Digital elevation model of Himachal Pradesh.

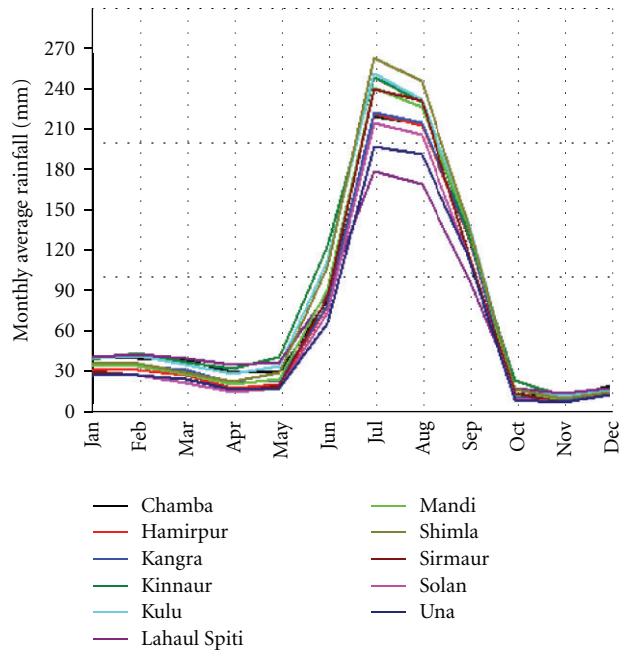

Figure 3: Monthly average rainfall variation in Himachal Pradesh.

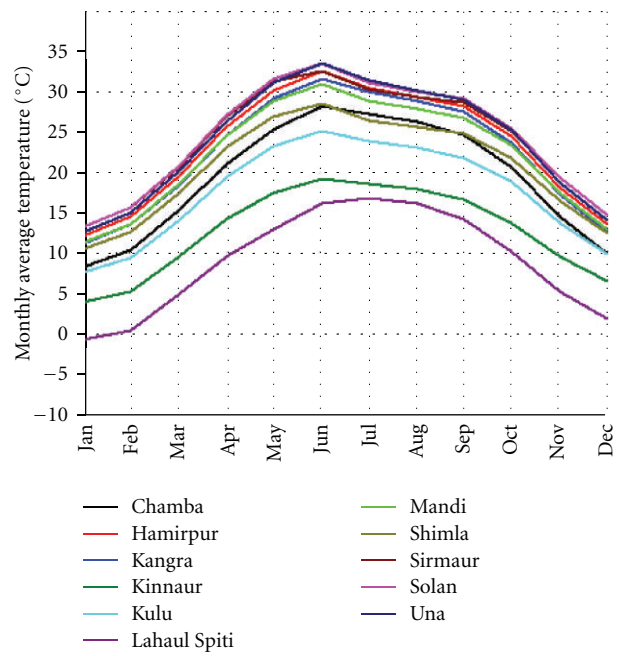

Figure 4: Monthly average temperature variation in Himachal Pradesh.

alpine zones with very sparse rainfall. The digital elevation model (DEM) based on 90 m resolution SRTM data (http://www2.jpl.nasa.gov/srtm/) along with district boundaries of the state provides clearer understanding of its topography (Figure 2).

The spatial and monthly variations of average rainfall (Figure 3) and temperature (Figure 4) over Himachal Pradesh have been observed from a 100 years meteorological dataset. The monthly average temperature decreases with altitude and shows a regional difference of approximately 15°C from higher elevations (above 3500 m) to lower (below 1000 m). Winter season commences in the month of October, reaches its peak in January, and continues till February. The months of March, April, May, and June are comparatively warmer. Figure 3 clearly shows the onset of Southwest monsoon in June with average rainfall uniformly reaching higher values in all the regions. The highest annual average rainfall is recorded in the district of Kinnaur and the least in Una. The rainfall slows down towards the end of September marking the end of the southwest monsoon season.

3.2. Availability of Surface Insolation Data. IMD has an ordinary solar radiation station in Himachal Pradesh which is situated in Manali at 32.27° North latitude and 77.17° East longitude measuring GHI. The data from the station do not suffice for a higher temporal- and spatial-scale study of solar energy availability throughout the state. Hence, larger spatiotemporal resolution satellite-derived solar resource datasets were collected, scrutinized, and validated for the study region.

4. Data, Models, and Methodology

4.1. NASA SSE

4.1.1. Data. Surface meteorology and solar energy (SSE) datasets provided by the National Aeronautics and Space Administration (NASA) Langley Research Center derive solar radiation and meteorological data from a variety of earth-observing satellites. The SSE Release 6.0 (accessible at http://gewex-srb.larc.nasa.gov/) provides 1°× 1° (∼100 × 100 km) spatial-resolution data on a global grid with temporal coverage of solar radiation parameters for 22 years from July 1st, 1983 to June 30th, 2005 obtained from daily 3 hourly satellite measurements for UTC (coordinated universal time) 0, 3,

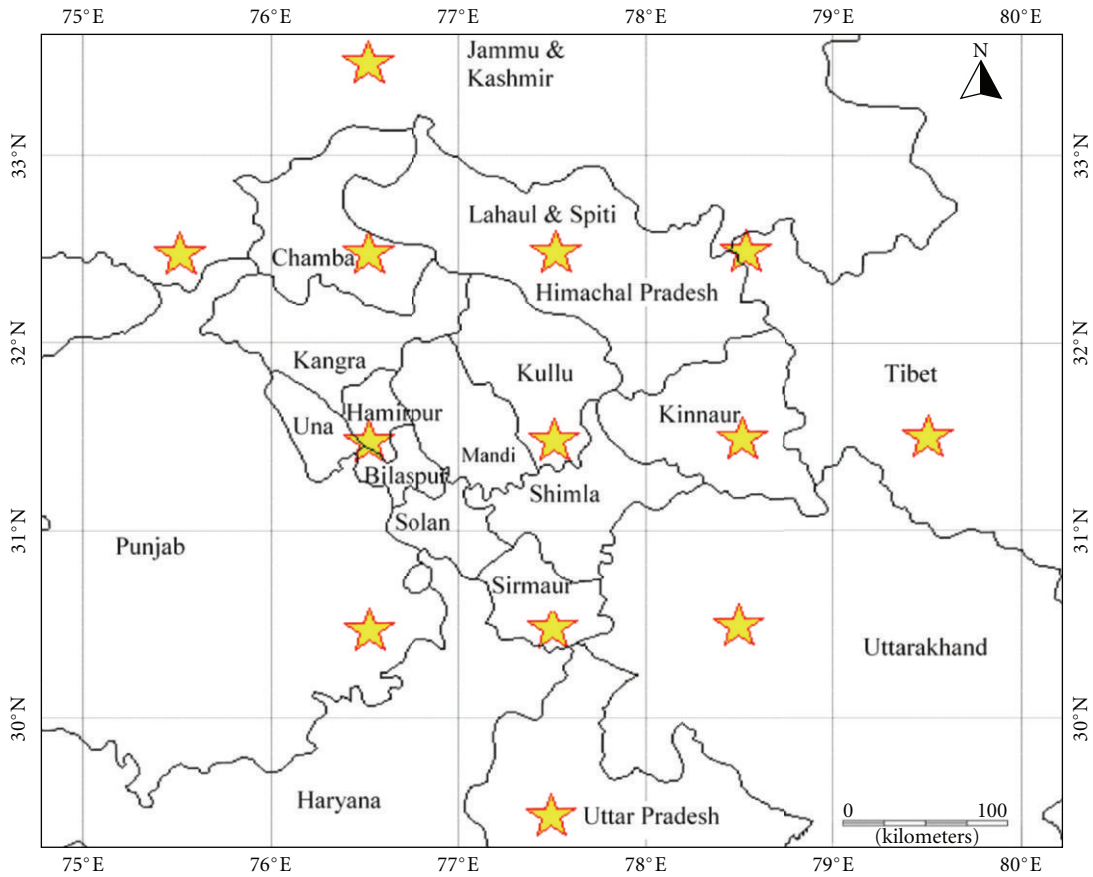

Figure 5: Selected grids (star marked) for procuring NASA SSE GHI data of Himachal Pradesh.

6, 9, 12, 15, 18, 21 hrs. The GHI data are available as daily, monthly, and annual averages [5].

4.1.2. Model. The NASA SSE solar dataset was derived from a physical model based on the radiative transfer theory which states that the solar radiation incident on the earth's surface is a result of absorption, scattering, and reflection of the sun's incoming radiation. The model demands precise knowledge of solar geometry, satellite calibration, and atmospheric composition. It employs a modeled atmosphere along with parameterization of its absorption and scattering properties. Primary inputs to the model include visible and infrared radiation, inferred cloud and surface properties, temperature, precipitable water, column ozone amounts and atmospheric state variables such as temperature and pressure [28]. The parameters were measured using instruments like CERES (clouds and the earth's radiant energy system), MODIS (moderate-resolution imaging spectro radiometer), TOMS (total ozone mapping spectrometer), and so forth mounted on GMS, NIMBUS, METEOR, GOES, METEOSAT, NOAA, and multifarious satellites. Insolation at a given location on the earth's surface was inferred based on the shortwave (0.2 to 4 μm) and longwave (4 to 100 μm) solar radiation reflected to the satellite sensors from the top of atmosphere (TOA). A calculative TOA solar radiation was iteratively compared to the values measured by the satellite sensors. Iterations were carried on parameters like aerosol distribution until the error was within a marginal value. GHI on the surface for each such iteration was computed for different durations [5].

4.1.3. Validation. Shortwave and longwave solar radiation datasets were derived based on primary algorithms by Pinker and Lazlo [29] and Fu et al. [30], respectively. The quality check algorithms called the Langley parameterized shortwave algorithm (LPSA) and downward longwave algorithm by Gupta et al. [31, 32] validates the primary algorithms. All the released datasets in SSE have undergone validation based on these four algorithms [33]. The derived solar radiation parameters were validated with baseline surface radiation network (BSRN) and RMSE of 10.25% were observed for GHI. The meteorological parameters were validated with information from the National Climate Data Center (NCDC).

4.2. NREL SUNY

4.2.1. Data. The National Renewable Energy Laboratory (NREL) and the Atmospheric Sciences Research Center (ASRC) at the State University of New York (SUNY)/Albany

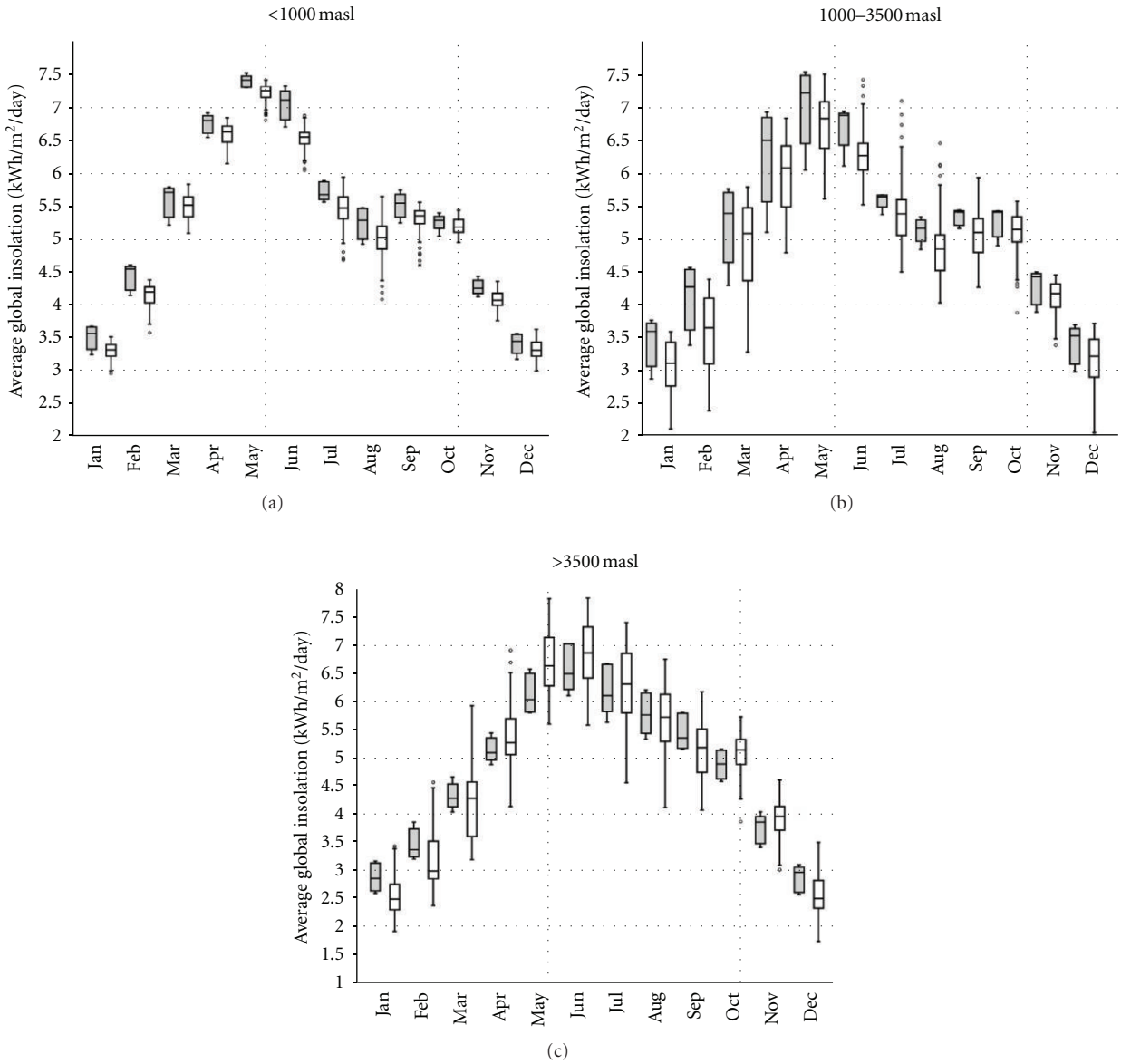

Figure 6: Comparison of monthly average GHI from NASA SSE (shaded box) and NREL SUNY (clear box) over different elevation zones (<1000 m, 1000–3500 m, >3500 m) of Himachal Pradesh.

developed satellite-based solar radiation data for India in collaboration with its Ministry of New and Renewable Energy (MNRE). They furnished $0.1^\circ \times 0.1^\circ$ ($\sim 10 \times 10$ km) higher-spatial-resolution data from half hourly satellite measurements of January 2002 to December 2008 made available in their web portal (http://www.nrel.gov/international/ra_india.html).

4.2.2. Model. The solar radiation data was derived from the SUNY satellite-to-irradiance model developed by Perez et al. [34]. This semiempirical model has characteristics of physical models (like that employed by NASA SSE) in addition to regression analyses on quality surface measurements. The model is based on the observation that shortwave atmospheric transmissivity is linearly related to the earth's planetary albedo captured as satellite image pixel counts. These image-pixels are normalized by the cosine of solar zenith angle, and location-specific cloud indices are generated. For each location, the GHI is derived from the cloud index based on extraterrestrial normal incident values, solar zenith angle, elevation, elevation-corrected air mass and certain additional parameters. The model output is fit to high-quality surface measurements at distinct geographic locations for correction and validation.

Apart from solar geometry and cloud cover, aerosol composition significantly influences the GHI. Aerosol optical depth (AOD), a unitless measure of the aerosol-induced solar attenuation, is considered as an indispensable input to the SUNY model. Reports of higher aerosol concentrations across India and studies on their temporal variability

Table 1: Solar radiation data through ground-based pyranometer [2].

Months	Jan	Feb	Mar	Apr	May	Jun	Jul	Aug	Sep	Oct	Nov	Dec	Annual
Average insolation (kWh/m^2/day)	3.55	4.19	5.32	6.33	7.10	6.5	5.48	5.81	5.33	5.20	4.00	3.23	5.17

demanded monthly AOD values to be inputted. These detailed AOD values were developed based on available satellite and ground data [35].

4.2.3. Validation. The SUNY model enhanced with analytical and numerical methods was employed for North and Central America. Later on, the methodology was adapted for Central Asia based on the European Meteosat 5 and 7 geostationary satellites. The model run for Northwest India was validated with measurements provided by IMD, NASA and SSE as well as NREL's ~40 km resolution climatological solar radiation (CSR) data. The SSE and CSR data were used for quality check of the 10 km NREL SUNY data [36]. The model enhanced with monthly AOD values and adopted for the entire geography of the country needs further validation with quality-controlled ground measurements.

5. Data Procurement and Comparison

The 1°× 1° resolution NASA SSE monthly averages of GHI for the study region were collected. Within a grid of ~10000 km^2 area, any points which do not lie on its northern or eastern boundaries share a common GHI value corresponding to the midpoint of the grid. Out of 13 optimal grids, 10 provide a complete coverage of the land area of the state while the other 3 are used to support an optimal interpolation through the geographic information system (GIS). Among all, 6 grids cover Chamba, Lahaul Spiti, Krishnaganj/Kinnaur, Hamirpur, Kullu, and Sirmaur districts of Himachal Pradesh, 5 grids cover the districts of Kargil, Kathua (Jammu & Kashmir), Fatehgarh Sahib (Punjab), Muzaffarnagar (Uttar Pradesh), and Tehri Garhwal (Uttarakhand), and 2 grids cover the Tibetan region (Figure 5). The NREL SUNY data cover an average area of 95.185 km^2 per grid in the study region. The monthly averages of GHI for 610 optimum grids covering the entire state of Himachal Pradesh were collected. This provides higher spatial resolution information preferable for regional-level potential assessment within the state.

The collected datasets from the NASA SSE and the NREL SUNY were compared and validated for three different elevation zones namely, <1000 m, 1000–3500 m, and >3500 m as shown in Figure 6. The monthly variations of average GHI were comparable for different elevation gradients. The RMSE of monthly average GHI between the NASA and the NREL datasets were 0.24, 0.32, and 0.28 kWh/m^2/day for <1000 m, 1000–3500 m, and >3500 m zones, respectively. NASA SSE-based GHI values were observed to be positively biased to the NREL SSE GHI data. These datasets were also validated with a reliable surface measurement [2] given in Table 1, showing RMSE of 0.25 kWh/m^2/day with NASA SSE and 0.38 kWh/m^2/day with NREL SUNY data. The relatively lower-resolution NASA SSE data were used to generate GHI maps for the entire state. This helps in identifying the regional and seasonal variability of GHI within the state. The higher-resolution NREL SUNY data were used for district-level GHI maps of the state essentially to quantify the regional potential for solar applications design.

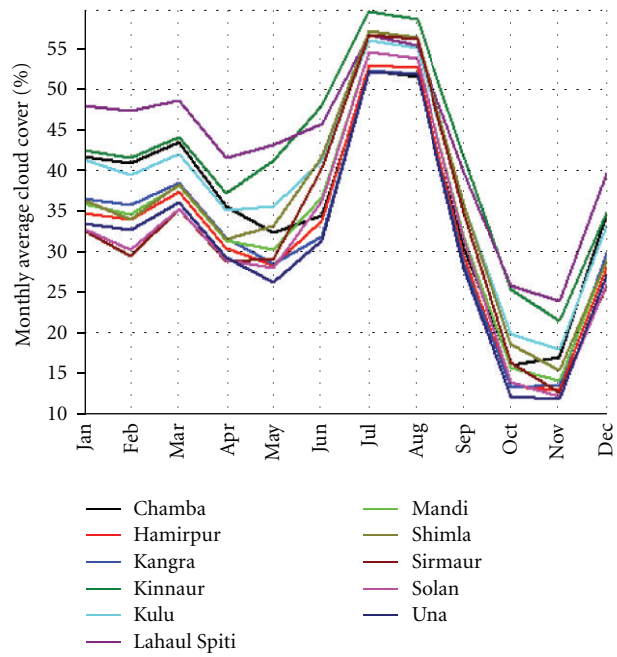

Figure 7: District wise monthly average cloud cover (%) in Himachal Pradesh.

6. Results and Discussion

6.1. Seasonal Variability of GHI: Geographic and Climatic Influences. The NASA and the NREL datasets were analysed spatially using GIS. Results based on both datasets show that Himachal Pradesh receives an average insolation of 5.86 ± 1.02–5.99 ± 0.91 kWh/m^2/day in the warm summer months of March, April, and May; 5.69 ± 0.65–5.89 ± 0.65 kWh/m^2/day in the wet monsoon months of June, July, August, and September; 3.73 ± 0.91–3.94 ± 0.78 kWh/m^2/day in the colder winter months of end October, November, December, January, and February. It is observed that the period from March to October which covers the summer and monsoon seasons over the entire agro-climatic zones of Himachal Pradesh receives insolation above 4 kWh/m^2/day. The insolation throughout Himachal Pradesh drops down with the onset of winter by the end of October, and a low insolation period prevails till the end of February.

Cloud cover increases with increasing elevation as a consequence of the cloud-topography interactions and orographically induced convection. This is evident from the

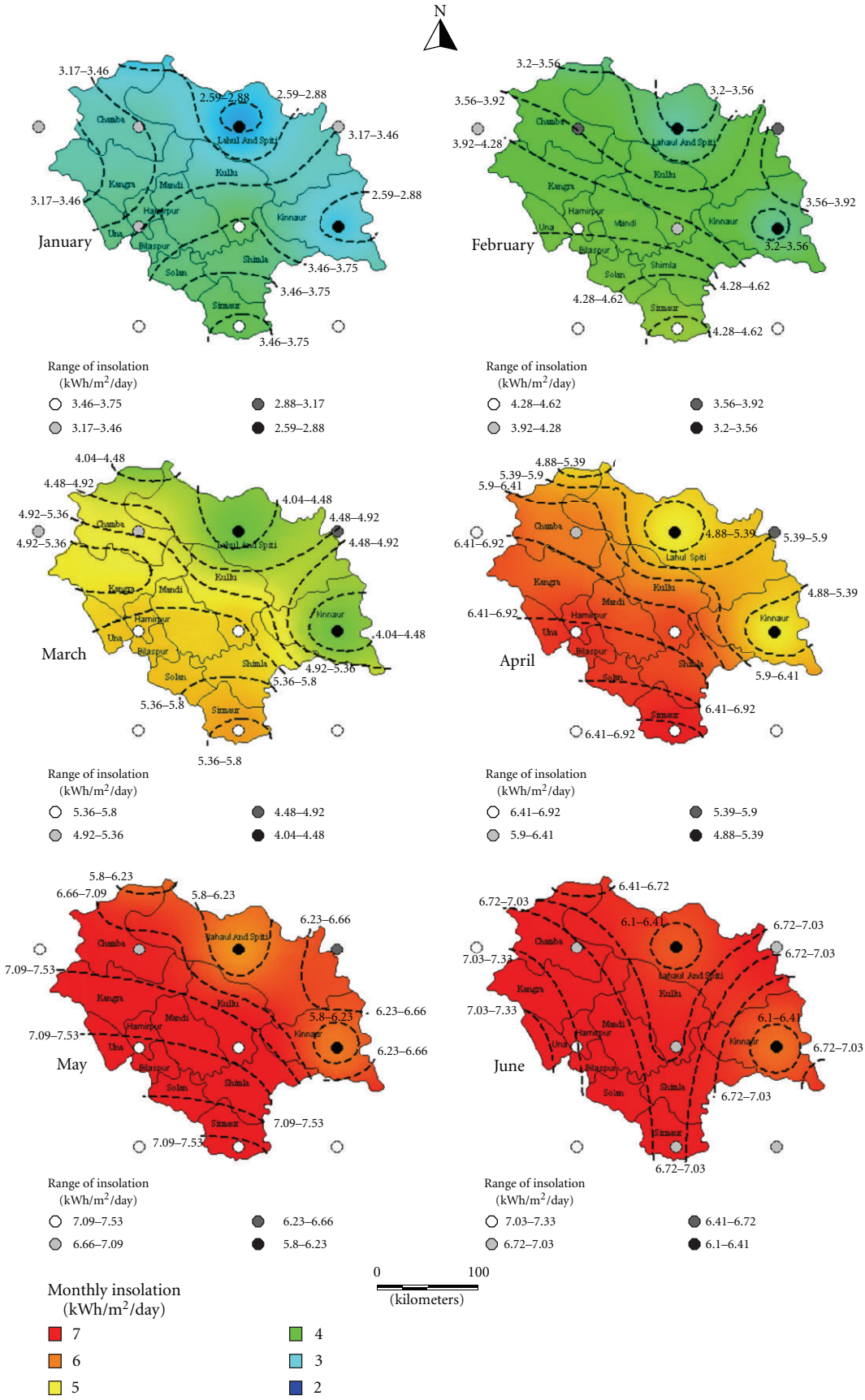

Figure 8: Monthly average GHI maps based on the NASA SSE data enriched with isohels for January–June.

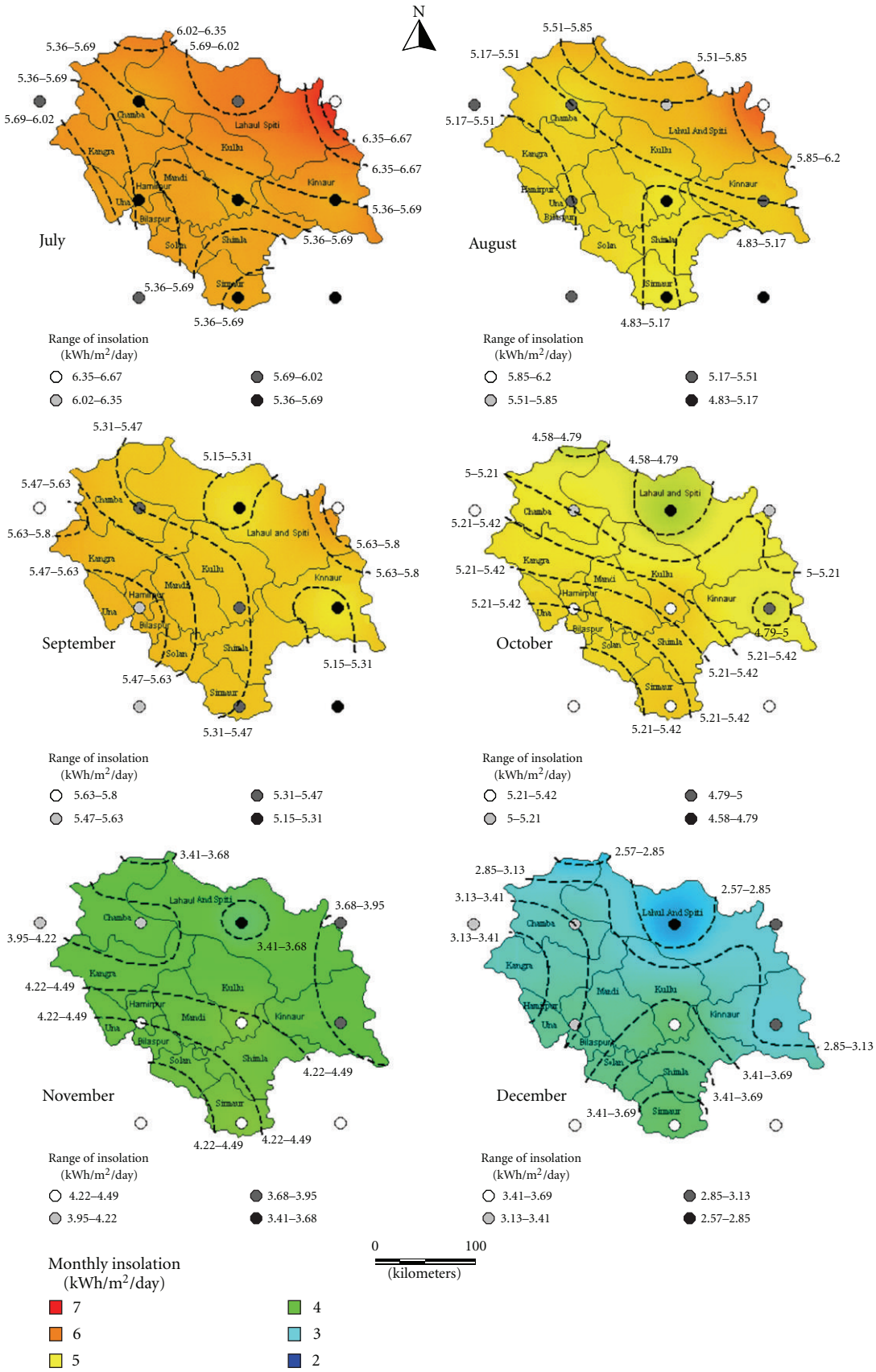

Figure 9: Monthly average GHI maps based on the NASA SSE data enriched with isohels for July–December.

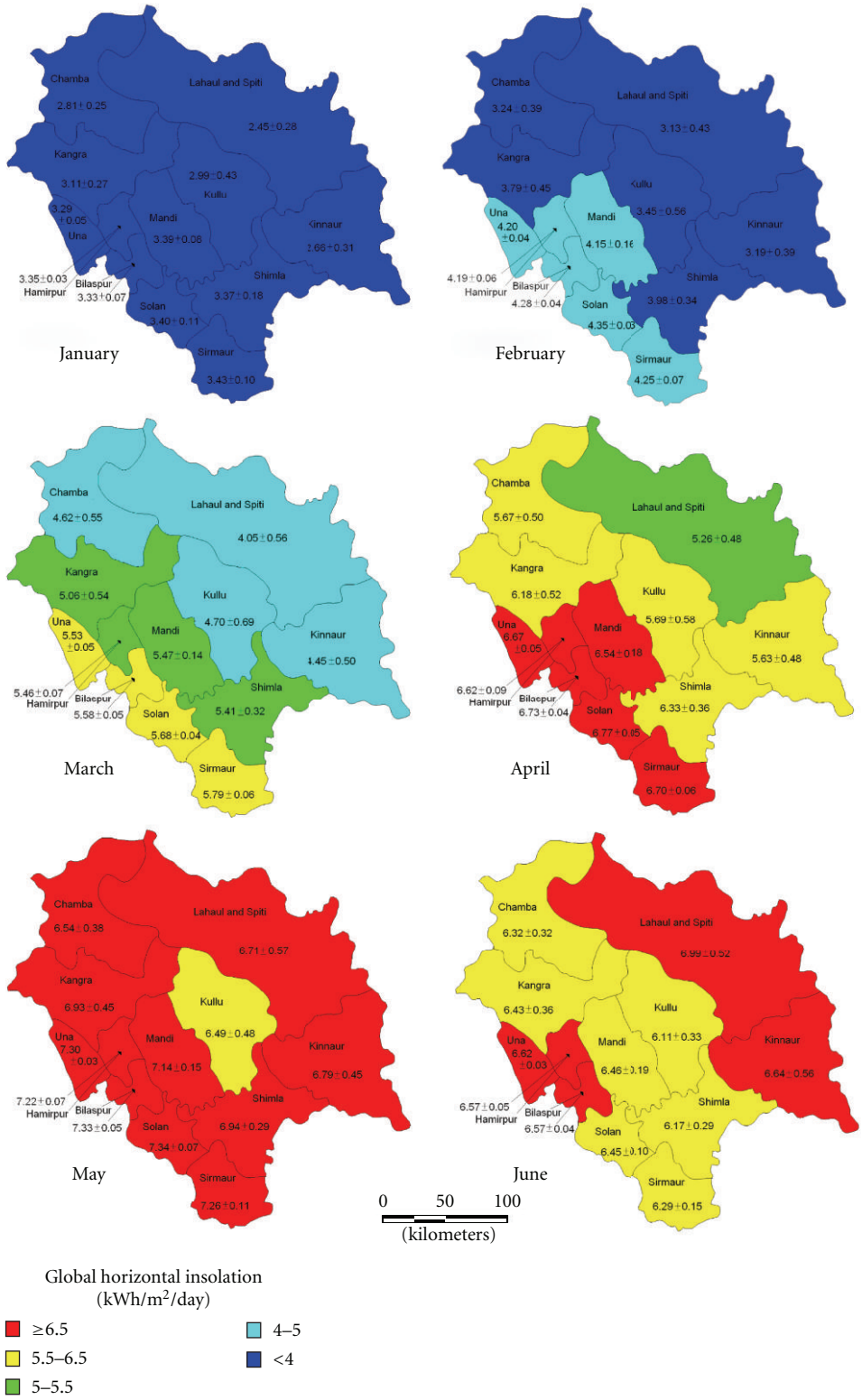

Figure 10: Monthly average district-level GHI maps based on the NREL SUNY data for January–June.

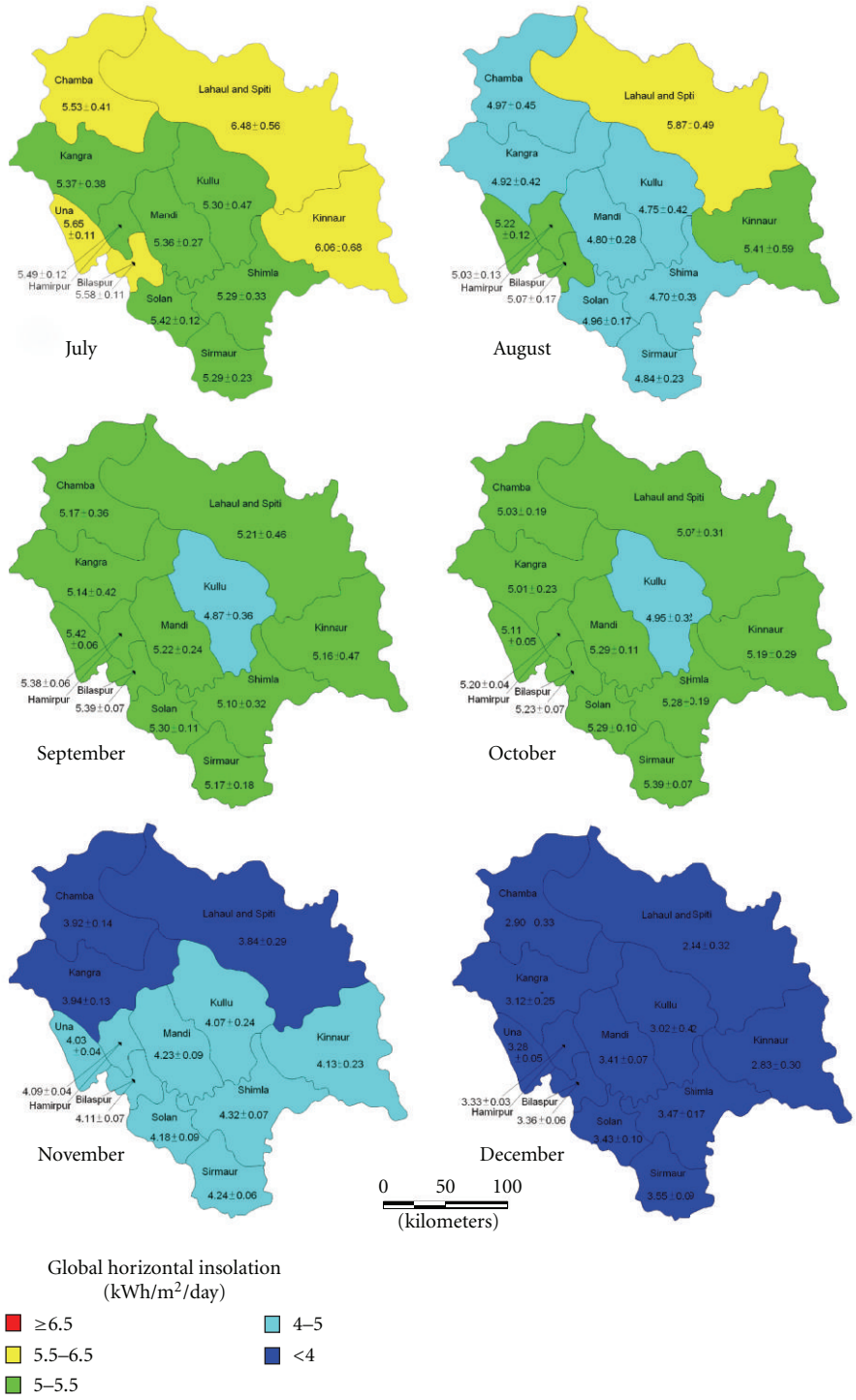

Figure 11: Monthly average district-level GHI maps based on the NREL SUNY data for July–December.

monthly average cloud cover data procured from a 100 years average meteorological dataset (Figure 7). The Lahaul Spiti district in the high-altitude alpine zone has the highest-average cloud cover, and the Solan district in the low-altitude tropical zone has the least. This also highlights the fluctuation in cloud amount over the advection facing and opposite sides of the mountains [37]. The relief and resultant cloud cover influences the regional variation in insolation to a bigger extent and are apparent in the box plots given in Figure 6. The insolation in Himachal Pradesh is observed

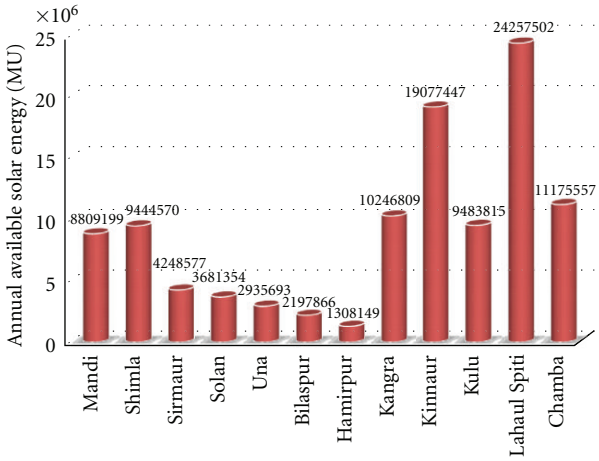

Figure 12: Annual available solar energy (in million units) in the districts of Himachal Pradesh.

to increase from high-altitude cold and dry alpine zone to the low-altitude warmer regions (below 1000 m). This regional insolation variation is observed for a major part of the year from October to May. However, the trend reverses from June to September with the high-altitude zone receiving comparatively higher insolation. These trends could be attributed to the Southwest monsoon and the increase in cloud cover over the low as well as middle-altitude regions (below 3500 m) and the northeast dry monsoon winds from Central Asia setting in October.

6.2. Regional Variability of GHI: Solar Resource Availability and Utilization. The monthly GHI maps based on NASA SSE enriched with isohels (regions receiving same amount of insolation) show the regional variability of the solar resources in Himachal Pradesh (Figures 8 and 9). The results are validated by the district-level monthly GHI maps generated based on the NREL SUNY data (Figures 10 and 11). The monthly solar resource availability as well as variability in different districts of Himachal Pradesh is noted. It is observed that the lower- and middle-altitude (<3500 m) districts of Una, Bilaspur, Hamirpur, Solan, Mandi, Sirmaur, and Shimla receive annual average GHI above 5 kWh/m^2/day. The districts of Lahaul Spiti, Kinnaur, Kullu, and Chamba located at higher altitude (>3500 m) receive annual average GHI in the range 4.5–5 kWh/m^2/day. As pointed in Section 6.1, the entire state receives monthly average GHI above 4 kWh/m^2/day from March to October. The lower and middle-altitude districts receive monthly average GHI above 4 kWh/m^2/day in the winter months of November and February, 3–3.5 kWh/m^2/day in December and January. However the entire winter witnesses least values ranging from 2.5 to 3 kWh/m^2/day in the higher-altitude districts.

The state of Himachal Pradesh consumed 5814 million kWh (or million units, MU) of electricity in 2009-2010 [38] giving us an estimate of the power requirement in the state. Analyses based on the NREL SUNY data show that Himachal Pradesh receives 99530395MU of solar energy per year. Figure 12 shows the district-wise annual average solar energy received. Considering 0.1% of the total land area in low- and middle-altitude districts available for solar energy utilization, 43324 MU is available annually for conversion through solar applications. Higher-altitude districts with sparse and isolated population require decentralized energy. The annually available solar energy of 56206 MU (considering 0.1% of the land area per district) could be effectively utilized along with additional energy sources as hybrids.

7. Conclusion

The NASA SSE and the NREL SUNY datasets available in user-friendly formats based on time tested and realistic models provided solar radiation data on higher spatial and temporal scales. The GHI datasets were collected, compared, validated, and represented using GIS for the complex terrain of Himachal Pradesh. Spatial analysis of these data aided in quantifying the solar potential in the hill state with scanty surface measurements even in the district level. It is observed that Himachal Pradesh receives annual average GHI above 4.5 kWh/m^2/day. The regional variations in GHI are influenced by its diverse topography as well as seasons. The lower- and middle-elevation zones (<3500 m) receive relatively higher GHI for a longer duration annually. However, the entire state receives considerably large amount of solar energy as demonstrated. Solar photovoltaic applications with reasonable efficiencies and costs are viable options. These could substantially improve the energy scenario by providing decentralized energy in the isolated and inaccessible pockets. The solar maps also provide necessary information for meteorology-, climatology-, agriculture-, and forestry-related studies. The approach is replicable to other complex terrains of the world and the study confirms the prospects for solar-based technologies to meet the impending energy crisis.

Acknowledgments

The authors thank the NASA and NREL for making available the solar datasets for renewable energy potential assessment throughout the world. They also thank the India Water Portal for providing 100 years district wise meteorological data for India. They are grateful to NRDMS division, the Ministry of Science and Technology, Government of India, and the Indian Institute of Science for the financial and infrastructure support.

References

[1] V. V. N. Kishore, *Renewable Energy Engineering and Technology: A knowledge Compendium*, TERI Press, New Delhi, India, 2008.

[2] A. Mani, *Handbook of Solar Radiation*, Allied Publishers, New Delhi, India, 1981.

[3] World Radiation Data Centre, St.Petersburg, August 2011, http://wrdc.mgo.rssi.ru/.

[4] R. D. Varshita and M. K. Gupta, *Modernisation of Radiation Network*, Indian Meteorological Department, Pune, India, 2010.

[5] NASA, Surface Meteorology and Solar Energy Release 6.0 Methodology, July 2010, http://eosweb.larc.nasa.gov/sse/documents/SSE6Methodology.pdf.

[6] A. Ortega, R. Escobar, S. Colle, and S. L. de Abreu, "The state of solar energy resource assessment in Chile," *Renewable Energy*, vol. 35, no. 11, pp. 2514–2524, 2010.

[7] C. A. Gueymard and D. R. Myers, "Evaluation of conventional and high-performance routine solar radiation measurements for improved solar resource, climatological trends, and radiative modeling," *Solar Energy*, vol. 83, no. 2, pp. 171–185, 2009.

[8] R. Pitz-Paal, G. Norbert, H.-K. Carsten, and S. Christoph, How to get bankable meteodata? DLR solar resource assessment, NREL 2007 parabolic trough technology workshop, Golden, Colorado, August 2010, http://www.nrel.gov/csp/troughnet/pdfs/2007/pitz_paal_dlr_solar_resource_assessment.pdf.

[9] T. V. Ramachandra and D. K. Subramanian, "Potential and prospects of solar energy in Uttara Kannada, district of Karnataka state, India," *Energy Sources*, vol. 19, no. 9, pp. 945–988, 1997.

[10] K. Yang, T. Koike, and B. Ye, "Improving estimation of hourly, daily, and monthly solar radiation by importing global data sets," *Agricultural and Forest Meteorology*, vol. 137, no. 1-2, pp. 43–55, 2006.

[11] X. Liu, X. Mei, Y. Li et al., "Evaluation of temperature-based global solar radiation models in China," *Agricultural and Forest Meteorology*, vol. 149, no. 9, pp. 1433–1446, 2009.

[12] D. L. Liu and B. J. Scott, "Estimation of solar radiation in Australia from rainfall and temperature observations," *Agricultural and Forest Meteorology*, vol. 106, no. 1, pp. 41–59, 2001.

[13] J. S. G. Ehnberg and M. H. J. Bollen, "Simulation of global solar radiation based on cloud observations," *Solar Energy*, vol. 78, no. 2, pp. 157–162, 2005.

[14] T. V. Ramachandra, "Solar energy potential assessment using GIS," *Energy Education Science and Technology*, vol. 18, no. 2, pp. 101–114, 2007.

[15] A. Sözen and E. Arcaklioğlu, "Solar potential in Turkey," *Applied Energy*, vol. 80, no. 1, pp. 35–45, 2005.

[16] C. M. Kishtawal, Meteorological Satellites, Satellite Remote Sensing and GIS Applications in Agricultural Meteorology, 2010, http://www.wamis.org/agm/pubs/agm8/Paper-4.pdf.

[17] A. Q. Malik, A. Mufti, H. W. Hiser, N. T. Veziroglu, and L. Kazi, "Application of geostationary satellite data for determining solar radiations over Pakistan," *Renewable Energy*, vol. 1, no. 3-4, pp. 455–461, 1991.

[18] J. E. Hay, "Satellite based estimates of solar irradiance at the earth's surface-I. Modelling approaches," *Renewable Energy*, vol. 3, no. 4-5, pp. 381–393, 1993.

[19] C. Sorapipatana, "An assessment of solar energy potential in Kampuchea," *Renewable and Sustainable Energy Reviews*, vol. 14, no. 8, pp. 2174–2178, 2010.

[20] J. Polo, L. F. Zarzalejo, M. Cony et al., "Solar radiation estimations over India using Meteosat satellite images," *Solar Energy*, vol. 85, no. 9, pp. 2395–2406, 2011.

[21] S. Tanahashi, H. Kawamura, T. Matsuura, T. Takahashi, and H. Yusa, "Improved estimates of hourly insolation from GMS S-VISSR data," *Remote Sensing of Environment*, vol. 74, no. 3, pp. 409–413, 2000.

[22] E. Cogliani, P. Ricchiazzi, and A. Maccari, "Generation of operational maps of global solar irradiation on horizontal plan and of direct normal irradiation from Meteosat imagery by using SOLARMET," *Solar Energy*, vol. 82, no. 6, pp. 556–562, 2008.

[23] S. Janjai, P. Pankaew, and J. Laksanaboonsong, "A model for calculating hourly global solar radiation from satellite data in the tropics," *Applied Energy*, vol. 86, no. 9, pp. 1450–1457, 2009.

[24] T. V. Ramachandra, R. Jain, and G. Krishnadas, "Hotspots of solar potential in India," *Renewable and Sustainable Energy Reviews*, vol. 15, no. 6, pp. 3178–3186, 2011.

[25] R. Perez, R. Seals, and A. Zelenka, "Comparing satellite remote sensing and ground network measurements for the production of site/time specific irradiance data," *Solar Energy*, vol. 60, no. 2, pp. 89–96, 1997.

[26] P. Illera, A. Fernández, and A. Pérez, "A simple model for the calculation of global solar radiation using geostationary satellite data," *Atmospheric Research*, vol. 39, no. 1–3, pp. 79–90, 1995.

[27] Statistical Data of Himachal Pradesh upto 2009-10, Himachal Pradesh Planning Department, Govt. of Himachal Pradesh, August 2010, http://hpplanning.nic.in/Statistical data of Himachal Pradesh upto 2009-10.pdf.

[28] SRB Data and Information, Atmospheric Science Data Center, NASA, August 2010, http://eosweb.larc.nasa.gov/PRODOCS/srb/table_srb.html.

[29] R. T. Pinker and I. Laszlo, "Modeling surface solar irradiance for satellite applications on a global scale," *Journal of Applied Meteorology*, vol. 31, no. 2, pp. 194–211, 1992.

[30] Q. Fu, K. N. Liou, M. C. Cribb, T. P. Charlock, and A. Grossman, "Multiple scattering parameterization in thermal infrared radiative transfer," *Journal of the Atmospheric Sciences*, vol. 54, no. 24, pp. 2799–2812, 1997.

[31] S. K. Gupta, A. C. Wilber, D. P. Kratz, and P. W. Stackhouse Jr., "The langley parameterized shortwave algorithm (LPSA) for surface radiation budget studies," NASA/TP-2001-211272, 2001.

[32] S. K. Gupta, C. H. Whitlock, N. A. Ritchey, and A. C. Wilber, An Algorithm for Longwave Surface Radiation Budget for Total Skies, CERES ATBD Subsystem 4.6.3, August 2010, http://ceres.larc.nasa.gov/documents/ATBD/pdf/r2_2/ceres-atbd2.2-s4.6.3.pdf.

[33] NASA/GEWEX Surface Radiation Budget Project, August 2010, http://gewex-srb.larc.nasa.gov/.

[34] R. Perez, P. Ineichen, K. Moore et al., "A new operational model for satellite-derived irradiances: description and validation," *Solar Energy*, vol. 73, no. 5, pp. 307–317, 2002.

[35] National Renewable Energy Laboratory, Colorado, USA, September 2011, http://www.nrel.gov/international/docs/readme_india_solar_maps.txt.

[36] Solar resource assessment methodology for Bhutan, National Renewable Energy Laboratory, Colorado, United states, March 2012, http://www.nrel.gov/international/pdfs/ra_bhutan_solar_methods_final.pdf.

[37] A. Z. Kotarba, "Satellite-derived cloud climatology over high elevation areas based on circulation types: a 2007 analysis of the Tatra Mountains," *Physics and Chemistry of the Earth*, vol. 35, no. 9–12, pp. 462–468, 2010.

[38] Himachal Pradesh Finance Department, September 2011, http://himachal.nic.in/finance/ES_201011/EconomisSurvey-Eng1011.pdf.